A facile strategy to fabricate lignin-based thermoset alternative to formaldehyde-based wood adhesives

*Xiaoyu Shi[a], Shishuai Gao[a], Can Jin[a], Daihui Zhang[*a,b,c], Chenhuan Lai[b*],Chunpeng Wang[a,b], Fuxiang Chu[a,b], Arthur J Ragauskas [d,e,f,g], Mi Li [d*]*

a. Institute of Chemical Industry of Forest Products, Chinese Academy of Forestry (CAF), Jiangsu Province, No 16, Suojin Wucun, Nanjing 210042, China.

b. Jiangsu Co-Innovation Center of Efficient Processing and Utilization of Forest Resources, Nanjing Forestry University, Nanjing 210037, China.

c. Key Laboratory of Wood Material Science and Application, Ministry of Education; MOE Engineering Research Center of Forestry Biomass Materials and Energy, Beijing Forestry University, 100083, Beijing, China

d. Center for Renewable Carbon, School of Natural Resources, The University of Tennessee, Knoxville, TN 37996, USA

e. Department of Chemical and Biomolecular Engineering, University of Tennessee, Knoxville, TN, 37996, USA

f. Center for Bioenergy Innovation, Biosciences Division, Oak Ridge National Laboratory, Oak Ridge, TN, 37831, USA

g. Joint Institute for Biological Science, Oak Ridge National Laboratory, Oak Ridge, TN, 37831, USA

Keywords: Lignin, thermosets, wood adhesives, composites;

Abstract

The utilization of sustainable lignin to synthesize wood adhesives has attracted increasing attention in recent years. However, the facile fabrication of strong and environmentally friendly lignin-based adhesives with high lignin content remains a significant challenge. This study developed a formaldehyde-free wood adhesive system by combining alkali lignin and poly(propylene glycol) bis(2-aminopropyl ether). The process of producing the lignin-based adhesives involves a simple mixing of wood flour, lignin, and commercially available crosslinker (polyetheramine), followed by directly hot-pressing into particleboards. The formaldehyde-free and non-toxic particleboards showed high biomass content of 75% and internal bonding strength of 1.42 MPa, outperforming many other bio-based adhesives. The study demonstrates a new and facile strategy to synthesize a lignin-based thermoset that is readily and practically applicable as adhesives to fabricate high-performance, high lignin content, and formaldehyde-free wood products.

1. Introduction

Wood composite panels are widely used in construction, flooring, and furniture. A wood adhesive plays a critical role in the manufacture of wood-based products. At present, most commercial wood adhesives are dominated by non-renewable fossil-derived polymers, such as melamine-formaldehyde (MF), urea-formaldehyde (UF), poly(vinyl acetate), polymeric diphenylmethane diisocyanate (pMDI) resin, and phenol-formaldehyde (PF)[1, 2], owing to their outstanding bonding performance and low cost. However, these petroleum resources-based resins face two serious challenges: (i) most will release certain levels of free formaldehyde, causing environmental and human health hazards; and (ii) the production of these resins heavily relies on non-renewable fossil resources. Therefore, it is vital to develop formaldehyde-free adhesives from biomass resources.

Over the past few decades, numerous natural biopolymers have been used as promising candidates for synthesizing bio-based wood adhesives[3-6]. Lignin has a phenolic structure and is one of the most widespread renewable natural polymers.[7, 8] However, lignin is generally considered a low-value by-product of lignocellulose biorefining during biomass pretreatments.[9] Although lignin as a precursor has the potential to synthesize wood adhesives[10], the economic and high-efficient utilization of lignin remains a challenge. It is widely accepted that lignin has a relatively low reactivity and complex structures, such as the molecular weight varying significantly with the sources and isolation methods[11-13]. These drawbacks significantly limited their effective utilization and practical applications.

Currently, two main strategies have been reported to fabricate lignin-based thermosets as wood adhesives. One common strategy lies in the additional chemical modification of lignin, such as hydroxymethylation[14, 15], phenolation[16], demethylation[17, 18], and depolymerization[19, 20], which is required to improve the reactivity of lignin. Ai *et al.*[15] reported a phenolic adhesive formulated *via* methylolation and alkalification-activated lignin. Unfortunately, these processes are cumbersome and energy-intensive. Another strategy involved directly incorporating unmodified lignin into commercial resins, such as PF resin. Sun *et al.*[21] prepared lignin–phenol–formaldehyde resin adhesives using biorefinery technical lignins. However, compared to the adhesive without lignin, the bonding strength of wood-based panels decreased upon the added amount of lignin in the resin, limiting the use of large amounts of lignin for wood adhesives[10]. Also, incorporating lignin into PF resin cannot entirely prevent the release of formaldehyde. Therefore, developing a formaldehyde-free wood adhesive with high lignin content is highly desired, but challenging.[3, 22]

Recently, Celzard *et al.*[23] investigated the reaction of condensed tannins with a diamine. The result showed that covalent and ionic bonds between the amine and the phenolic hydroxy groups of the tannin are formed at higher temperatures (at 180 °C), leading to polycondensed resins. Subsequently, Delmotte *et al*.[24] prepared polyurethanes using kraft lignin, hexamethylene diamine, and dimethyl carbonate without isocyanates, indicating the potential reaction between lignin and diamine. The above studies inspired us to believe that a direct combination of lignin and diamine could afford polymerization and prepare novel adhesives for the wood industry.

However, to the best of our knowledge, this has never been investigated. In this study, a formaldehyde-free wood-adhesive system consisting of alkali lignin and poly(propylene glycol) bis(2-aminopropyl ether) (D2000) was designed. The potential mechanism to form the lignin-based thermosets was investigated. In addition, their utilization as wood adhesives for bonding particleboards has been demonstrated. This study reports a facile strategy to prepare lignin-based wood adhesives to obtain formaldehyde-free and high lignin-content particleboards.

2. Experimental methods

2.1 Materials

Dezhou Longli (Shandong) Co. provided commercial alkali lignin, Ltd. Wood flour was provided by Dare Wood-Based Panel Group Co., Ltd. Poly(propylene glycol) bis(2-aminopropyl ether) (D2000, M_n =2000 g/mol, Sigma-Aldrich), p-toluenesulfonic acid (TsOH, 99.9%, Macklin) and 1,4-dioxane (99.9%, Sigma-Aldrich) were all used as received.

2.2 Preparation of lignin-based thermosets

To prepare lignin-based thermosets with different compositions, the catalyst TsOH (1 wt % of lignin) and different ratios of reactants (lignin over D2000) were added into a glass flask together with 1,4-dioxane addition to achieve a homogeneous resin. Specifically, alkali lignin (3.00 g), TsOH (0.03 g), and D2000 (2.25g) were mixed in 15 mL of dioxane. After stirring for 2 h at room temperature to completely dissolve lignin, the mixture were poured into PTFE molds, heated at 110 °C for 8 h to evaporate 1,4-dioxane, and then heated at 180 °C for 24 h to produce lignin-based thermoset resins.

The cured thermosets were denoted according to the ratio of alkali lignin to D2000. For example, LD 1:0.75 indicates that the weight ratio of alkali lignin to D2000 is 1 to 0.75. Thermosets with LD of 1:1, 1:1.5, and 1:2 were also prepared similarly.

2.3 Panel processing

Firstly, lignin and D2000 were mixed with wood flour in designed formulations (**Table S1**). After blending for 10 min, the mixtures were manually added into a wooden mold. Next, the mat was placed onto a hot press and pressed at 180 °C for 15 min with a pressure of 4.0 MPa.

2.4 Gel fraction measurement

The immersion method measured the gel fraction (G_f) of lignin-based resin. The lignin-based thermosets (W_1, ~0.5 g) were immersed in 20 mL of 1,4-dioxane at room temperature for 48 h, and the insoluble fraction was dried to a constant weight (W_2) in an oven at 80 °C for 16 h. The G_f of the sample was calculated as described by Eq. 1:

$$G_f = \frac{W_2}{W_1} \times 100\% \qquad (1)$$

2.5 Characterization

The Fourier Transform Infrared (FT-IR) spectra were recorded by a SPECTRUM 100 spectrophotometer (Perkin Elmer) from 4,000 to 600 cm^{-1} with a resolution of 4 cm^{-1} and a scanning number of 32 times. X-ray photoelectron spectroscopy (XPS) was used to analyze the chemical structure of the materials, which was recorded on a Thermo Fischer (America, ESCALAB) spectrometer using Al Kα excitation radiation (X-ray source powered at 20 mA and 15 kV) and a vacuum system of 8×10^{-10} mbar. NETZSCH Instruments DSC-214 obtained differential scanning calorimetry (DSC)

curve. The measurement was performed from -70 to 50 °C at a rate of 5 °C·min^{-1} under an N_2 atmosphere. Dynamic mechanical analysis (DMA) curves were recorded by DMA Q800 under tensile mode from -80 to 200 °C with a heating rate of 3 °C·min^{-1} and an oscillation frequency of 1 Hz. Thermogravimetric analysis (TGA) was tested on a NETZSCH TG 209F1 Libra equipment from 30 to 790 °C with a heating rate of 10 °C min^{-1} under an N_2 atmosphere. The cross-sectional view of the particleboards was observed through a field emission scanning electron microscope (SEM, JSM-7800 F) under 2.0 kV acceleration voltage. Samples were gold-coated in a vacuum sputter coater. The composition of lignin was determined by standard National Renewable Energy Laboratory (NREL) protocols. Quantitative ^{31}P NMR spectra of the lignin were acquired by a Bruker AVANCE 600 MHz spectrometer (see support information for details). Formaldehyde emission from the produced particleboards was measured using the desiccator method based on JIS A 1460: 2001 (see support information for details).

3. Results and discussion

3.1 Synthesis of lignin-based thermosets

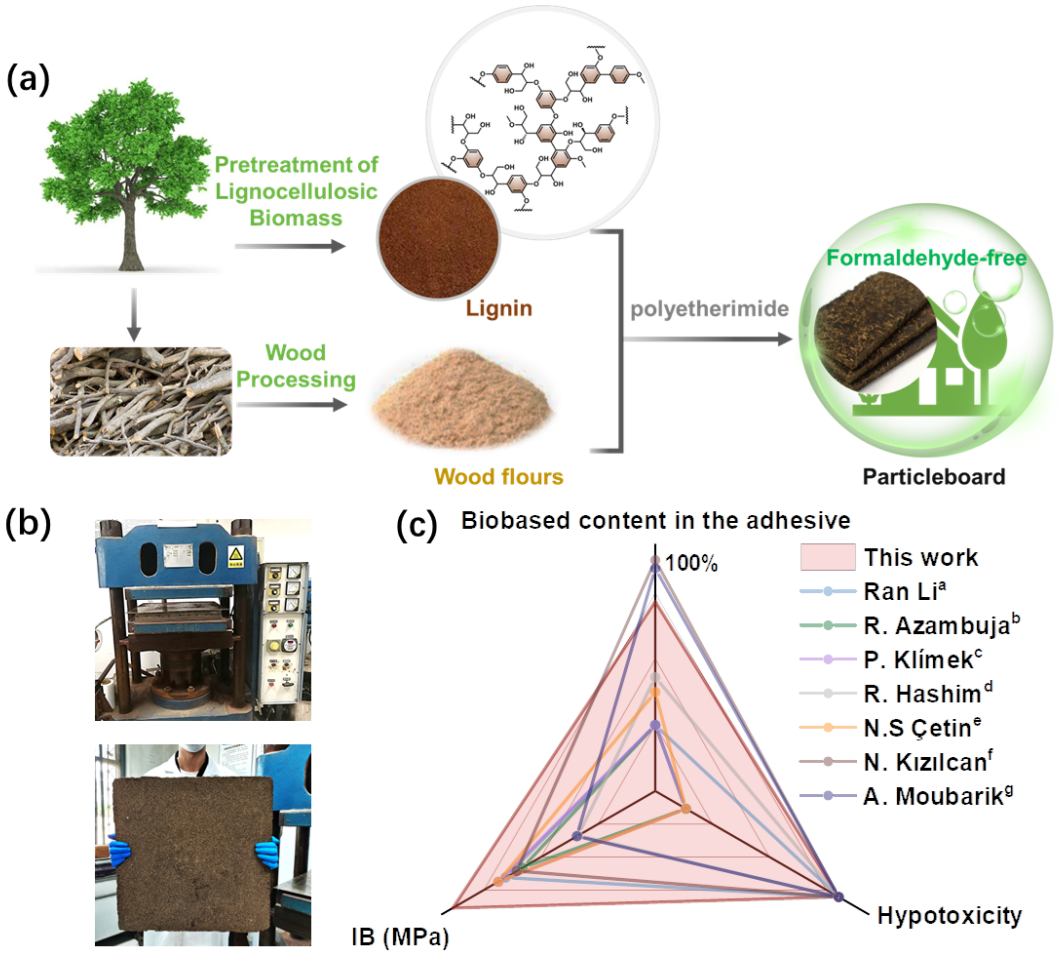

Figure 1. (a) Overview of the fabrication of form aldehyde-free particleboard from lignin. (b) The hot-pressing process and the image of the particleboards (500 mm ×500 mm ×7.5 mm). (c) This study compares the internal bonding (IB) strength, hypotoxicity, and biomass content of particleboards using sustainable adhesives to previously reported adhesives [25-31]. [an] Unsaturated polyester resin mixed with phenolic formaldehyde; [b] Urea formaldehyde resin; [c] Methylene diphenyl diisocyanate; [d] Carboxymethyl starch mixed with polyvinyl alcohol; [e] Cornstarch, mimosa tannin, sugar, and citric acid; [f] Carboxylated cellulose nanocrystals filled starch; [g] Lignin and phenol-formaldehyde resins.

The fabrication process of lignin-based adhesives and particleboard is shown in **Fig. 1a**. Unlike most previous studies that modify lignin to reactive precursors with complicated steps[32-35], the readily available wood flour, lignin and the commercially

available crosslinker (polyetheramine) were used without treatment or chemical modification. They could be simply mixed and directly hot-pressed to generate particleboards-a facile process in which lignin-based adhesive was synthesized simultaneously with no formaldehyde emission (**Fig. 1b**). Moreover, the fabrication of particleboards using this method could be easily dropped into the current wood-based board facilities and upscaled for practical applications. Large-size wood-flour particleboard of 500 mm ×500 mm ×7.5 mm is easily prepared in our lab (**Fig. 1b**). We conjectured that a covalently crosslinked network was formed by the direct reaction between lignin and polyetheramine during the hot compression leading to the particleboards with an unprecedented combination of extremely high internal bonding (IB) strength of 1.42 MPa, biomass content of 75% lignin, and hypotoxicity (i.e., formaldehyde-free). It is recognized that there are usually trade-offs among the mechanical strength, biomass content, and hypotoxicity to be achieved for the majority of bio-based adhesives reported to date (**Fig. 1c**)[25-31]. For example, Moubarik *et al*.[30] reported a particleboard using carboxylated cellulose nanocrystals filled starch-based adhesives. Although a similar biomass content was used (about 95%), the IB was only around 0.55 MPa. Cetin *et al*.[31] investigated particleboard using the lignin-phenol-formaldehyde adhesives. Although the IB was around 1.1 MPa, the biomass content was only around 30%. We have achieved the fabrication of high-lignin content particleboard with strong IB and low hypotoxicity using a straightforward approach.

3.2 Physicochemical properties of the lignin-based thermosets

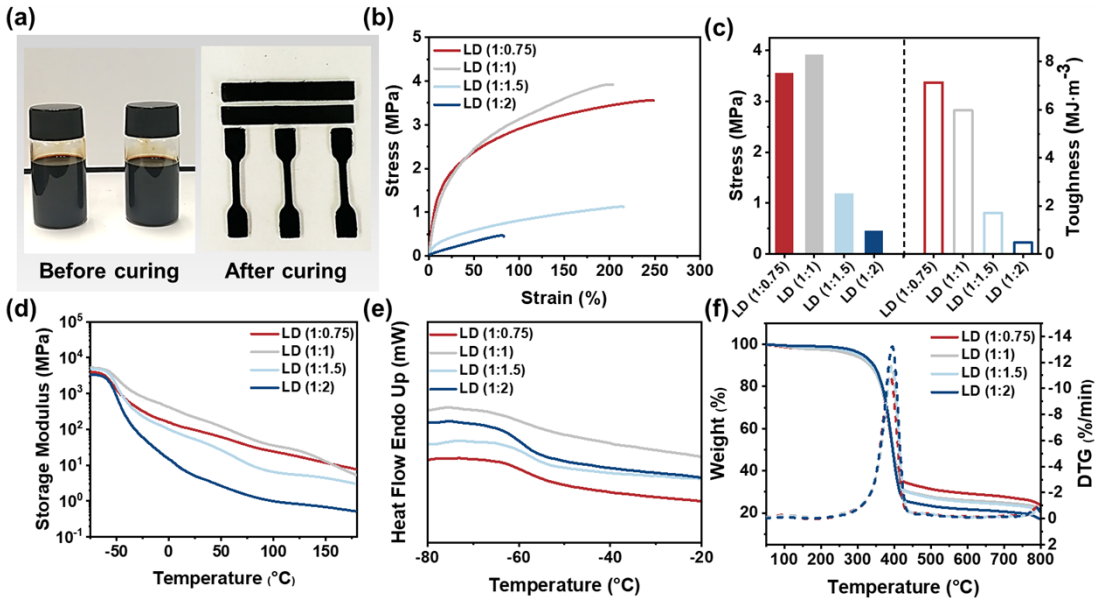

Figure 2. (a) Lignin-based thermosets before and after curing. (b) The tensile testing curves for the lignin-based thermosets. (c) Calculated tensile strengths and toughness of lignin-based thermosets. (d) Storage modulus versus temperature for the thermosets. (e) DSC and (f) TGA curves of lignin-based thermosets with different LD ratios.

First, four lignin-based thermosets with different ratios of alkali lignin to D2000 (from 33 to 50 wt %) were prepared to evaluate the effect of lignin to crosslinkers ratio on the physicochemical properties of thermosets. During the generation of lignin-based thermosets, we first tried a direct hot compression of the lignin and D2000 mixture without additional solvent, leading to a failure to obtain a homogeneous thermoset. This result might be due to the polyetheramine's poor dispersion and dynamic mass transportation of lignin. By contrast, a stable black thermoset could be afforded by dissolving lignin and polyetheramine in dioxane before hot compression **(Fig. 2a). Fig. 2b** showed the tensile stress–strain curves of the lignin-based thermosets, and all the lignin-based thermosets made with different LD ratios were very ductile with 82.9–248.5% elongation at break. In comparison to previously reported results for lignin-

based thermosets, our work exhibited relatively high elongation at break[36-38]. We believe that the structural flexibility of crosslinkers was the main reason providing the impressive tensile strain. However, both tensile strength and toughness varied along with the gradual increase in the crosslinker content. This fact was interrelated with the crosslinking density and the rigidity of the covalently crosslinked chains. For example, the stress and strain of LD (1:1.50) were 1.12 MPa and 215.3%, while LD (1:1) and LD (1:0.75) were tougher with the stress of 3.92 and 3.55 MPa, and strain of 203.6 and 248.5%, respectively. The addition of a large amount of D2000 potentially reduced the crosslink density and the stiffness of the thermoset **(Fig. 2b and 2c).** The gel content analysis confirmed the generation of crosslinked structures (**Table 1**), owing to the effective reaction between lignin and D2000. However, the crosslinking density initially increased and decreased as the lignin contents increased. When the lignin content was low, fewer active sites were available for the reaction with D2000, resulting in a lower network crosslink density. As the lignin content further increased, the number of active sites to react with D2000 increased, increasing the crosslink density. However, the excessive number of lignin addition would cause a decrease in the crosslink density owing to the poor reactions among lignins. Therefore, LD (1:1) has the highest crosslink density (310.79×10^{-3}mol m^{-3}). This trend was in agreement with the gel content and the strength variation.

Table 1. Physicochemical properties of the lignin-based thermosets with different compositions

sample	T_g (°C)[a]	T_g (°C)[b]	Er (MPa)[c]	V_e (10^{-3}mol m^{-3})[d]	Gel content (%)
LD (1:0.75)	-50.2	-58.3	269.37	128.09	72.2

LD (1:1)	-47.6	-60.1	660.32	310.79	81.3
LD (1:1.5)	-48.3	-58.4	170.69	80.24	69.3
LD (1:2)	-48.1	-59.7	33.90	15.82	61.1

[a] T_g was measured from the peak of tan δ peak based on DMA data; [b]T_g was obtained from DSC analysis; [c]Obtained by DMA data at T_g+30 °C; [d]The crosslinking density. (V_e) was calculated by the equation G(T) = RTV$_e$, where G is the rubber shear modulus, R is the universal gas constant, and T is the absolute temperature.

The changes in storage modulus and loss factor (tan δ) as a function of temperature are presented in **Fig 2d and Fig S1.** The modulus is usually related to the crosslinking density. As expected, the storage modulus initially increased and then decreased as the lignin contents increased at 25 °C (from 5.0 to 215.4 MPa). The T_g was also determined from the peak temperature of tan δ (**Fig S1**), and the peak maxima of tan δ at -50.2, -47.6, -48.3, and -48.1 °C were assigned as the T_g for LD (1:0.75), (1:1), (1:1.5), and (1:2), respectively. All lignin-based thermosets had low (< -45 °C) and similar glass transition temperatures, which were attributed to the excellent flexibility of D2000. Meanwhile, the T_g trend was consistent with the one observed by DSC **(Fig. 2e)**. **Fig. 2f** showed the thermal degradation of lignin-based thermosets in the range of 25 to 800 °C. All the lignin-based thermosets had excellent thermal stability, which was suggested by the onset degradation temperature (expressed as T_{d5}, temperature at 5% weight loss) (352.6–357.3 °C). All the TGA curves showed two major weight loss stages. The first one was situated between 60 and 120 °C, probably caused by the evaporation of water, while the second one, between 240 and 440 °C, was associated with the cleavage of lignin linkages.[39, 40] As the temperature continued to rise, the entire

lignin-based thermosets eventually decomposed to remain 17.18–23.87% of residual carbon. Overall, the lignin-based thermosets can withstand high temperatures of 350 °C and have good thermal stability.

3.3 Potential reaction mechanism of lignin-based thermosets synthesis

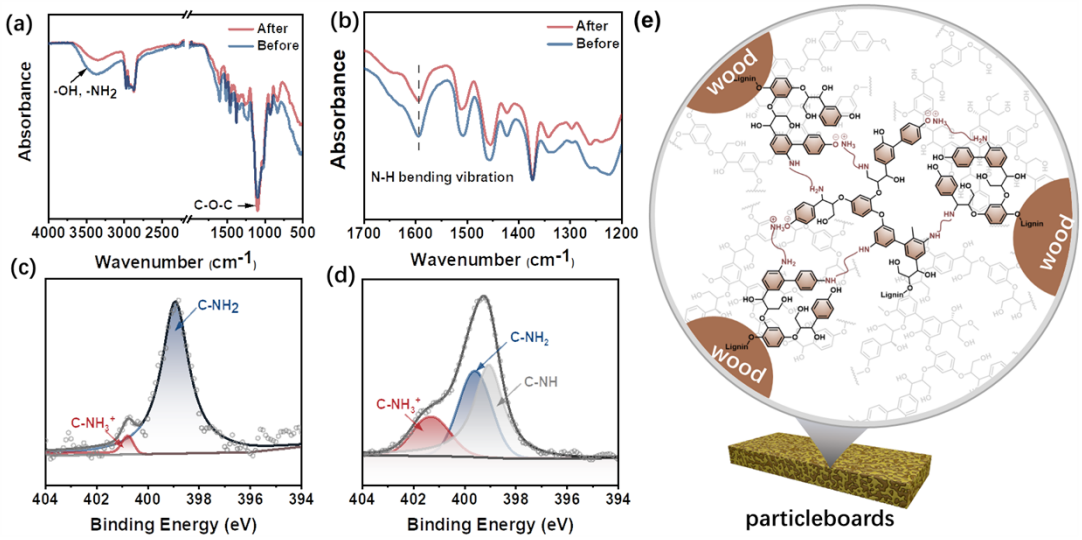

Figure 3. (a, b) FT-IR spectra of LD (1:1) before and after the cure. N 1s XPS spectra of samples before (c) and after (d) the cure. (e) Proposed mechanism for the lignin-based thermosets.

Previously, several potential mechanisms have been suggested regarding lignin-based reactions. For example, carbonium ions were formed in the lignin molecule under acidic wood treatments, which readily reacted with the strong nucleophile[41, 42]. In addition, Pizzi *et al.*[23, 24, 43] have observed the generation of ionic and covalent bonds between the amine and the phenolic hydroxy groups of tannin, leading to polycondensation resins. Recently, self-bonding of the lignin structures *via* radicals formation has also been demonstrated[44]. In order to reveal the potential reaction mechanism of lignin-based thermosets, several analyses were performed, including FTIR and XPS. The chemical structures of samples before and after the curing through

their FTIR spectra (**Fig. 3(a, b)**) clearly showed that the peaks at 3,200-3,450 cm^{-1} (hydroxyl and amino) and 1,590 cm^{-1} (−NH bending vibration) significantly decreased, suggesting that reactions between the amino groups of the crosslinker and the hydroxyl groups of the lignin occurred. Meanwhile, the peaks at 1,089 cm^{-1} attributed to the increase in the ether bonds,[45] due to condensation reactions between lignin molecules.[46] In the XPS analysis (**Fig. 3(c, d)**), the N 1s XPS of samples showed the content of -NH_2 decreased and the content of -NH and -NH_3^+ increased before and after the cure. These results indicate that there were both covalent and ionic bonds formed between amino groups in D2000 and hydroxyl groups in lignin.

3.4 Applications as Wood Adhesives

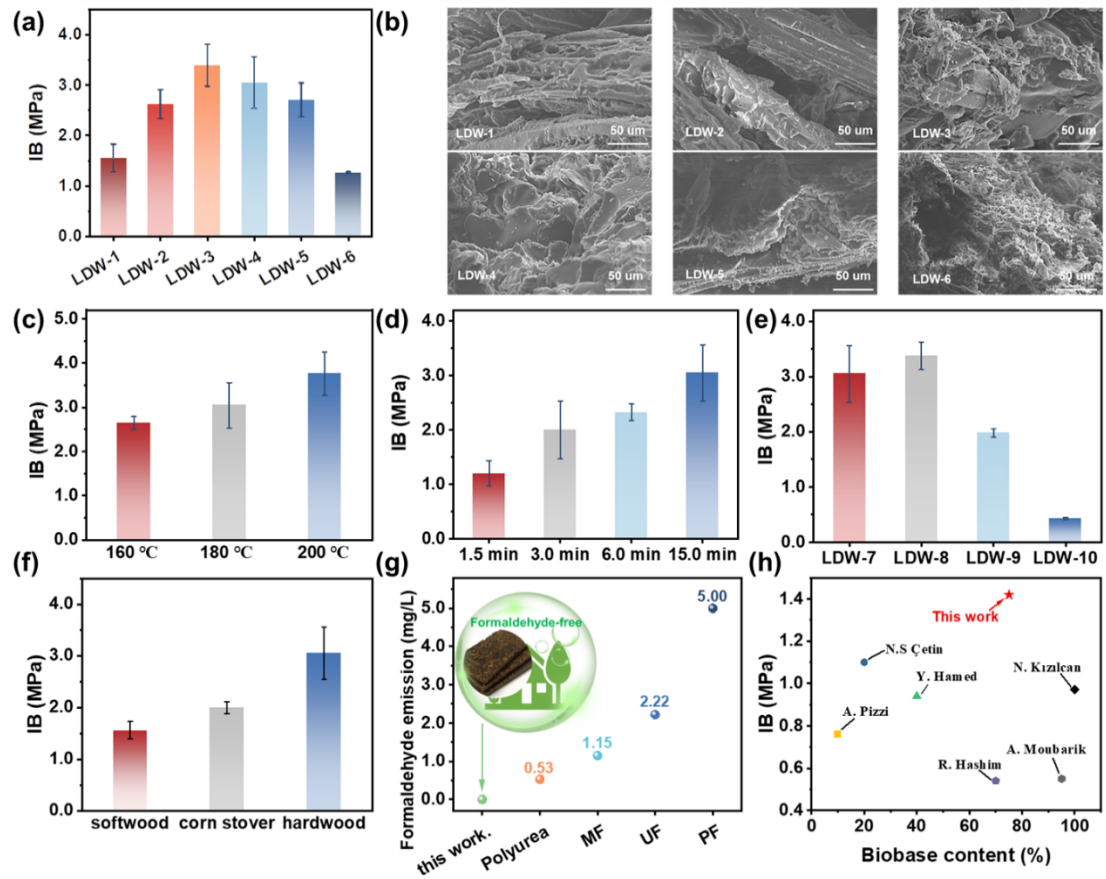

Figure 4. (a) The internal bonding strength of particleboards with different contents of D2000 (LDW-X, with "L" standing for lignin, "D" for D2000, "W" for wood flours, and the numbers "X" for sample number, see **Table S1** for details). (b) The cross-sectional view of the particleboards with different contents was observed through SEM. The internal bonding strength of particleboards with different hot-pressing temperatures (c), time (d), and different lignin content (e). (f) The internal bonding strength of particleboards with different lignin. (g) Comparison between adhesives presented herein and traditional adhesives in terms of formaldehyde emission. (h) Comparison between sustainable adhesives presented herein and previously reported adhesives regarding IB strength and biomass content[28-31, 47, 48].

The potential of using the lignin-based thermosets as formaldehyde-free wood adhesives were also demonstrated in this work. Lignin and D2000 were added in different proportions to wood flours (**Table S1**). All the particleboards fell in the range of high-density particleboards with a density range from 804 to 866 kg/m^3. **Table 3** exhibits the thickness swelling (TS) and water absorption (WA) values of the particleboards made from lignin-based thermosets. The TS and WA of LDW-6 (control sample) were 18.28% and 73.42%, respectively. However, after the addition of D2000, the TS values decreased within a range of 5.17%–16.79%. Similarly, WA values were decreased within a range of 50.04%–67.85%. These results indicated that D2000 improved the contact among the fine particles, which caused the closed structure of the board[49, 50]. Besides, the dispersion of the D2000 over the particleboards might also reduce water absorption since D2000 possessed a hydrophobic structure, contributing to the lower WA of the particleboards[51].

Table 3. Physical properties of particleboards.

Sample	Density (kg/m^3)	Thickness swelling (%)	Water absorption (%)
LDW-1	804.52±2.61	5.17±0.50	50.04±1.88
LDW-2	822.10±9.71	6.70±1.32	59.74±7.68
LDW-3	829.83±5.40	6.86±3.47	63.95±0.61
LDW-4	839.01±6.68	12.75±2.03	64.86±5.24
LDW-5	865.98±17.58	16.79±4.58	67.85±5.45
LDW-6	896.79±3.90	18.28±5.21	73.42±5.44

The internal bonding strength of the particleboard made with lignin-based thermosets were 1.2–3.3 MPa (**Fig. 4a**). The IB strength initially increased and then decreased as the contents of D2000 decreased. Without D2000 addition, the IB strength decreased to 1.2 MPa. The IB strength of particleboard was highly dependent on the crosslinking density of cured resin network[52]. The findings agreed with the crosslinking density of lignin-based thermosets (**Table 2**), and the addition of a large amount of D2000 reduced the crosslink density of the thermosets. Moreover, to evaluate the microstructure of the particleboards, the micrographs of cross-sections of the particleboards were observed by SEM (**Fig. 4b**). From the micrographs obtained through cross-section, the smoother surface of the wood flours was observed as the contents of D2000 increased. These results indicated that D2000 increased the connection between lignin and wood flours and improved the interfacial compatibility between these two materials.

In addition to the crosslinker ratio, the effect of hot-press temperature and time on IB strength was evaluated (**Fig. 4 c, d)**. The IB strength gradually increased from 2.7 to

3.7 MPa when the hot-press temperature increased from 160 to 200 °C. Similarly, the IB strength significantly increased from 1.3 to 3.2 MPa when the hot-press time increased from 1.5 to 15 min. This result suggests that by prolonging the hot-press duration and elevating the temperature, the resin adhesive can achieve a more thorough curing process. Hence, adjusting the hot-pressing conditions can easily modify the board's performance. We also investigated the effect of lignin content on the IB strength of particleboards (**Fig. 4e**). The IB strength initially increased and then decreased as lignin content decreased. With no lignin addition, the IB strength significantly decreased to 0.4 MPa. This result suggests that lignin in particleboards serves a similar role as in natural wood, acting as an adhesive that enhances the bonding strength between wood particles. Therefore, we explored the impacts of the lignin varieties in planta on particleboard performances. Corn stover, populus, and masson pine were selected in this research as representative feedstocks of herbaceous plants, hardwood, and softwood, respectively. As shown in **Fig. 4f**, the IB strength of the particleboards showed significant differences among hardwood, softwood, and herbaceous biomass. In particular, the IB strength of the particleboards made of lignin from populus (hardwood) was 3.0 MPa, which was higher than others from both corn stover (2.0 MPa, herbaceous plants) and Masson pine (1.5 MPa, softwood). By analyzing the components of the samples (**Table S2**). The results showed that the pure lignin content of Masson pine was the lowest (70.50%), which caused lower IB strength of the particleboards. However, the IB strength of the particleboards made from corn stover with the highest lignin content is lower than populus. In order to further reveal the

structural variations, the hydroxyl groups and molecular weight of populus and corn stover lignin were analyzed by quantitative ^{31}P NMR and gel permeation chromatography, respectively. As shown in **Table S3** and **Table S4**, although the hydroxyl groups of corn stover lignin (10.00 mmol/g) were higher than populus lignin (5.29 mmol/g), the molecular weight of corn stover lignin (3429 g/mol) was significantly lower than populus lignin (8669 g/mol). This comparison result indicated that the molecular weight of lignin was another dominant factor in improving the IB strength of particleboards. Larger molecular weight lignin has already provided specific crosslinking density to the network and,[53] in turn, enhances the IB strength.

According to the raw material ratio and hot-press conditions of LDW-4, we further enlarged the size of the particleboards to 500 mm ×500 mm ×7.5 mm (as shown in **Figure S3**) with a target density of 820 kg/m^3. The TA, WA, IB, modulus of rupture (MOR), and modulus of elasticity (MOE) for the particleboards are listed in **Table S5**. The formaldehyde was not detected by a desiccator method (**Fig. 4g**). In comparison to previously reported results for particleboards (**Fig. 4h**), the studied particleboards exhibited high biobased content and excellent IB strength.

4. Conclusions

This study investigates the use of a formaldehyde-free wood adhesive system made of alkali lignin and poly(propylene glycol) bis(2-aminopropyl ether) (D2000) to prepare particleboards. During the hot-pressing process, the lignin and D2000 form crosslinked networks containing ionic bonds and covalent bonds, leading to particleboards with high internal bonding strength, high biomass content, and low

toxicity. The IB strength, MOR, and MOE for the particleboards were 1.42 MPa, 16.74 MPa, and 1831.80 MPa, respectively. Previous studies using bio-based adhesives have faced challenges in achieving high biomass content and IB strength, but this study outperforms those reported to date. Although the comprehensive properties of particleboards need to be further improved, this facile strategy shows its potential to fabricate formaldehyde-free, high-lignin-content wood adhesives in the future.

Conflicts of interest

There are no conflicts to declare.

Acknowledgments

We acknowledge the support from the National Natural Science Foundation (32001283, 32271809, and 31890774) and the Fundamental Research Funds for the Central Nonprofit Research Institution of the Chinese Academy of Forestry (CAFYBB2021QB004).

References

1. P. V. Dhawale, S. K. Vineeth, R. V. Gadhave, J. Fatima M. J, M. V. Supekar, V. K. Thakur and P. Raghavan, *Materials Advances*, 2022, **3**, 3365-3388.
2. F. Ferdosian, Z. Pan, G. Gao and B. Zhao, *Journal*, 2017, **9**.
3. R. J. Li, J. Gutierrez, Y.-L. Chung, C. W. Frank, S. L. Billington, and E. S. Sattely, *Green Chemistry*, 2018, **20**, 1459-1466.
4. C. Wei, X. Zhu, H. Peng, J. Chen, F. Zhang and Q. Zhao, *ACS Sustainable Chemistry & Engineering*, 2019, **7**, 4508-4514.
5. H. Yin, P. Zheng, E. Zhang, J. Rao, Q. Lin, M. Fan, Z. Zhu, Q. Zeng and N. Chen,

Carbohydrate Polymers, 2020, **250**, 116884.

6. P. Zheng, N. Chen, S. M. Mahfuzul Islam, L.-K. Ju, J. Liu, J. Zhou, L. Chen, H. Zeng and Q. Lin, *ACS Sustainable Chemistry & Engineering*, 2019, **7**, 3909-3916.
7. A. Vinod, H. Pulikkalparambil, P. Jagadeesh, S. M. Rangappa and S. Siengchin, *Heliyon*, 2023, e13614.
8. X. Lu and X. Gu, *International Journal of Biological Macromolecules*, 2023, **229**, 778-790.
9. X. Chen, Z. Li, L. Zhang, H. Wang, C. Qiu, X. Fan and S. Sun, *Industrial Crops and Products*, 2021, **164**, 113396.
10. C. Huang, Z. Peng, J. Li, X. Li, X. Jiang, and Y. Dong, *Industrial Crops and Products*, 2022, **187**, 115388.
11. X. Song, S. Tang, X. Chi, G. Han, L. Bai, S. Q. Shi, Z. Zhu and W. Cheng, *ACS Sustainable Chemistry & Engineering*, 2022, **10**, 11655-11665.
12. B. M. Upton and A. M. Kasko, *Chemical Reviews*, 2016, **116**, 2275-2306.
13. J. A. Poveda-Giraldo, J. C. Solarte-Toro and C. A. Cardona Alzate, *Renewable and Sustainable Energy Reviews*, 2021, **138**, 110688.
14. D. Schieppati, A. Dreux, W. Gao, P. Fatehi and D. C. Boffito, *Journal of Cleaner Production*, 2022, **366**, 132776.
15. S. Feng, T. Shui, H. Wang, X. Ai, T. Kuboki and C. C. Xu, *Industrial Crops and Products*, 2021, **161**, 113225.
16. X. Jiang, J. Liu, X. Du, Z. Hu, H.-m. Chang and H. Jameel, *ACS Sustainable Chemistry & Engineering*, 2018, **6**, 5504-5512.

17. X. Yang, Z. Li, L. Li, N. Li, F. Jing, L. Hu, Q. Shang, X. Zhang, Y. Zhou and X. Pan, *Journal of Agricultural and Food Chemistry*, 2021, **69**, 13568-13577.

18. Z. Li, E. Sutandar, T. Goihl, X. Zhang and X. Pan, *Green Chemistry*, 2020, **22**, 7989-8001.

19. Z. Sun, B. Fridrich, A. de Santi, S. Elangovan and K. Barta, *Chemical Reviews*, 2018, **118**, 614-678.

20. X. Xiao, Y. Han, C. Liu, Y. Li, G. Sun and X. Wang, *Materials Today Sustainability*, 2023, **21**, 100317.

21. S. Yang, Y. Zhang, T.-Q. Yuan and R.-C. Sun, *Journal of Applied Polymer Science*, 2015, **132**.

22. M. Siahkamari, S. Emmanuel, D. B. Hodge and M. Nejad, *ACS Sustainable Chemistry & Engineering*, 2022, **10**, 3430-3441.

23. F. J. Santiago-Medina, A. Pizzi, M. C. Basso, L. Delmotte and A. Celzard, *Polymers (Basel)*, 2017, **9**.

24. F. J. Santiago-Medina, M. C. Basso, A. Pizzi and L. Delmotte, *Journal of Renewable Materials*, 2018, **6**, 413-425.

25. R. Li, C. Lan, Z. Wu, T. Huang, X. Chen, Y. Liao, L. Ye, X. Lin, Y. Yang, Y. Zheng, Y. Xie, and Q. Zhuang, *Construction and Building Materials*, 2017, **148**, 781-788.

26. R. d. R. Azambuja, V. G. de Castro, R. Trianoski and S. Iwakiri, *Journal of Building Engineering*, 2018, **20**, 488-492.

27. P. Klímek, R. Wimmer, P. Meinlschmidt and J. Kúdela, *Industrial Crops and Products*, 2018, **111**, 270-276.

28. J. Lamaming, N. B. Heng, A. A. Owodunni, S. Z. Lamaming, N. K. A. Khadir, R. Hashim, O. Sulaiman, M. H. Mohamad Kassim, M. H. Hussin, Y. Bustami, M. H. M. Amini and S. Hiziroglu, *Composites Part B: Engineering*, 2020, **183**.

29. S. Oktay, N. Kızılcan and B. Bengü, *Industrial Crops and Products*, 2021, **170**, 113689.

30. A. Ait Benhamou, A. Boussetta, Z. Kassab, M. Nadifiyine, H. Sehaqui, M. El Achaby and A. Moubarik, *Construction and Building Materials*, 2022, **348**, 128683.

31. N. S. Çetin and N. Özmen, *International Journal of Adhesion and Adhesives*, 2002, **22**, 481-486.

32. K. A. Henn, S. Forssell, A. Pietiläinen, N. Forsman, I. Smal, P. Nousiainen, R. P. Bangalore Ashok, P. Oinas and M. Österberg, *Green Chemistry*, 2022, **24**, 6487-6500.

33. Y. Chen, H. Zhang, Z. Zhu, and S. Fu, *International Journal of Biological Macromolecules*, 2020, **152**, 775-785.

34. X. Chen, X. Xi, A. Pizzi, E. Fredon, G. Du, C. Gerardin and S. Amirou, *The Journal of Adhesion*, 2021, **97**, 873-890.

35. M. M. Rahman, M. H. Zahir and H. D. Kim, *Journal*, 2016, **8**.

36. Y. Xu, K. Odelius and M. Hakkarainen, *ACS Applied Polymer Materials*, 2020, **2**, 1917-1924.

37. C. Gioia, G. Lo Re, M. Lawoko and L. Berglund, *Journal of the American Chemical Society*, 2018, **140**, 4054-4061.

38. S. Zhang, T. Liu, C. Hao, L. Wang, J. Han, H. Liu and J. Zhang, *Green Chemistry*, 2018, **20**, 2995-3000.

39. A. Moreno, M. Morsali and M. H. Sipponen, *ACS Appl Mater Interfaces*, 2021, **13**, 57952-57961.

40. M. J. Gan, Y. Q. Niu, X. J. Qu and C. H. Zhou, *Green Chemistry*, 2022, **24**, 7705-7750.

41. J. Li, G. Henriksson and G. Gellerstedt, *Bioresource Technology*, 2007, **98**, 3061-3068.

42. T. Pielhop, G. O. Larrazábal and P. Rudolf von Rohr, *Green Chemistry*, 2016, **18**, 5239-5247.

43. F. J. Santiago-Medina, A. Pizzi, M. C. Basso, L. Delmotte and S. Abdalla, *Journal of Renewable Materials*, 2017, **5**, 388-399.

44. B. Jiang, C. Chen, Z. Liang, S. He, Y. Kuang, J. Song, R. Mi, G. Chen, M. Jiao and L. Hu, *Advanced Functional Materials*, 2020, **30**, 1906307.

45. C. Liu, B. Yuan, M. Guo, Q. Yang, T. T. Nguyen and X. Ji, *Advanced Composites and Hybrid Materials*, 2021, **4**, 1176-1184.

46. W. Schutyser, T. Renders, S. Van den Bosch, S. F. Koelewijn, G. T. Beckham and B. F. Sels, *Chemical Society Reviews*, 2018, **47**, 852-908.

47. H. Younesi-Kordkheili and A. Pizzi, *Polymers (Basel)*, 2021, **13**.

48. H. Younesi-Kordkheili, *International Journal of Adhesion and Adhesives*, 2022, **113**, 103080.

49. A. Ghani, Z. Ashaari, P. Bawon and S. H. Lee, *Building and Environment*, 2018, **142**, 188-194.

50. G. Han, C. Zhang, D. Zhang, K. Umemura and S. Kawai, *Journal of Wood Science*, 1998, **44**, 282-286.

51. E. Y. Nakanishi, M. R. Cabral, P. d. S. Gonçalves, V. d. Santos and H. Savastano Junior, *Journal of Cleaner Production*, 2018, **195**, 1259-1269.

52. K. Siimer, T. Kaljuvee, P. Christjanson and I. Lasn, *Journal of Thermal Analysis and Calorimetry*, 2006, **84**, 71-77.

53. M. E. Jawerth, C. J. Brett, C. Terrier, P. T. Larsson, M. Lawoko, S. V. Roth, S. Lundmark and M. Johansson, *ACS Applied Polymer Materials*, 2020, **2**, 668-676.